Quantum size effect on dielectric function of ultrathin metal film: a first-principles study of Al(1 1 1)

Quantum size effect on dielectric function of ultrathin metal film: a first-principles study of Al(1 1 1)

Wenmei Ming[1], Steve Blair[2] and Feng Liu[1]

[1] Department of Materials Science and Engineering, University of Utah, 201 Presidents Cir, Salt Lake City, UT 84112, USA
[2] Department of Electrical and Computer Engineering, University of Utah, 201 Presidents Cir, Salt Lake City, UT 84112, USA

E-mail: fliu@eng.utah.edu

Abstract

Using first-principles calculations, we show manifestations of the quantum size effect in the dielectric function ε_2 of free-standing Al(1 1 1) ultrathin films of 1 monolayer to 20 monolayers, taking into account size dependent contributions from both interband and intraband electronic transitions. Overall the in-plane components (interband transition) of ε_2 increase with film thickness at all frequencies, converging towards a constant value. However, the out-of-plane components of ε_2 show a more complex behavior, and, only at frequencies less than 0.75 eV, increase with film thickness without convergence. This suggests that ultrathin films can possibly be used for low-loss plasmonics devices in the visible and ultraviolet range. Our findings may shed light on searching for low-loss plasmonic materials via quantum size effect.

Keywords: quantum size effect, ultrathin metal film, optical dielectric function

(Some figures may appear in colour only in the online journal)

1. Introduction

When the size of a material (in one, two or all three dimensions) is reduced to nanoscale, its properties become size dependent due to the quantum confinement effect or the surface effect, where the former is generally referred to as the quantum size effect (QSE) [1]. In recent years, there have been intensive studies of QSE on properties of ultrathin films in the quantum confinement regime. In particular, when the thickness of a metal film is comparable with the electron Fermi wavelength, quantum confinement becomes prominent, resulting in discretization of electronic states (quantum-well states). This in turn leads to a variety of strongly thickness-dependent film properties, manifested as QSE, such as surface energy [2, 3], surface stress [4, 5], surface diffusion barrier [6, 7], surface reactivity [8], work function [9], elastic constant [10] and so on.

Furthermore, considering the field of plasmonics [11–13] for myriad applications, the QSE is expected to also affect the plasmonic properties through varying the dielectric function of ultrathin metal films. Theoretically, Dryzek *et al* [14] and Apell *et al* [15, 16] showed QSE on the optical spectra of gold and potassium thin films, respectively, with a finite free electron model, which differs from the classical Drude model. Laref *el al* [17] studied the thickness dependence of the optical permittivity of ultrathin gold films for a more accurate design of plasmonic device based on density functional theory (DFT) calculation. Experimentally, Kuzik *et al* [18, 19] observed the periodic oscillation of optical conductivity as a function of film thickness in Nb, Cu, Mo, W, Ni and Ti, which is possibly an indication of QSE.

Because simple metals such as Ag, Au, Cu, Al and Mg have high electron density of states around the Fermi level, they have large bulk Drude plasma frequencies ω_{pl} of about 10 eV. The real part of dielectric function $\varepsilon(\omega)$ in the classical Drude model is $\varepsilon(\omega) = 1 - \omega_{pl}^2/\omega^2$, hence it is negative for frequencies up to Drude plasma frequency. The surface plasmon, formed at the interface between metal (negative $\varepsilon(\omega)$)

and a dielectric material (positive $\varepsilon(\omega)$), is proportional to the Drude plasma frequency, and hence may have frequencies over a wide range up to the visible and ultraviolet (UV). However, one problem with using these metals is the large energy loss of the applied electromagnetic field, largely because these metals are not ideal free electron gases and have interband electronic transitions under irradiation. The energy absorption from the interband electronic transitions falls also into the visible and UV range [11, 20]. Band structure engineering, therefore, is required to remove the interband transitions or push them out of visible and UV range, especially for visible and UV plasmonic applications. One interesting idea is to reduce the thickness of the metal films so that one may take the advantage of QSE to reduce absorption in the frequency range of interest. This idea has motivated the present study of QSE on the dielectric properties of ultrathin Al(1 1 1) films.

We have investigated the QSE on the dielectric function of free-standing Al(1 1 1) films with both interband and intraband contributions in the thickness range from 1 monolayer (ML) to 20 MLs, using first-principles DFT calculations within the random phase approximation (RPA) [21]. This approach has been used to successfully study the optical properties of low dimensional structures, such as nanotubes [22], graphene systems [23] and nanowires [24]. Overall the in-plane components (interband transition) of ε_2 increase with film thickness at all frequencies ,converging towards a constant value. However, the out-of-plane components of ε_2 show a more complex behavior, and, only at frequencies less than 0.75 eV, increase with film thickness but without convergence. This suggests that ultrathin films can possibly be used for low-loss plasmonics devices in the visible and UV range.

2. Calculation details and theory

Our DFT calculations were performed by using the projector augmented wave pseudopotential [25], with the generalized gradient approximation [26] to the exchange-correlation functional, with VASP package [27]. A free-standing Al(1 1 1) slab, plus a more than 20 Å vacuum, was used as our model film structure. 350 eV energy cutoff and $61 \times 61 \times 1$ Γ-centered k-mesh were used for wavefuntion expansion and k-space integration, respectively, to achieve a highly converged dielectric function. The internal atomic coordinates of all the films were relaxed using conjugate gradient method until the force exerted on each atom is smaller than 0.01 eV Å^{-3}. The in-plane lattice constant of 2.857 Å for Al(1 1 1) film was used. For a better bulk reference, we used a hexagonal unit cell with three Al(1 1 1) layers without vacuum, and the same energy cutoff and in-plane k-point sampling as the slab calculation to determine the bulk Al dielectric function.

The dielectric function of a metal has contributions from interband and intraband transitions. The former is in the form of a 2nd rank tensor and its imaginary part is expressed as [21]:

$$\varepsilon_{\alpha\beta}^{2,\text{inter}}(\omega) = \frac{8\pi^2 e^2}{\Omega m^2 \omega^2} \sum_{n \neq m; k} (f_{mk} - f_{nk}) P_{e_\alpha; m, n, k} P_{e_\beta; m, n, k} \delta \\ \times (\epsilon_{mk} - \epsilon_{nk} - \omega) \qquad (1)$$

where Ω is the volume of the unit cell, f_{nk} is Fermi–Dirac occupation function, e_α is the unit Cartesian directional vector of electric field polarization, and ϵ_{nk} is the electron eigen-energy. $P_{e_\alpha; m, n, k}$ is the momentum matrix element between the Bloch wavefunctions of (m, k) and (n, k) with projection onto the e_α direction. The corresponding real part can be computed through the Kramers–Kronig relation.

The intraband-transition dielectric function $\varepsilon_{\alpha\beta}^{2,\text{intra}}(\omega)$ has the Drude form with intraband Drude plasma frequency $\omega_{\text{pl};\alpha\beta}^2(\omega)$ below:

$$\varepsilon_{\alpha\beta}^{2,\text{intra}}(\omega) = \frac{\Gamma \omega_{\text{pl};\alpha\beta}^2}{\omega(\omega^2 + \Gamma^2)}. \qquad (2)$$

$$\omega_{\text{pl};\alpha\beta}^2 = \frac{8\pi^2 e^2}{\Omega m^2} \sum_{n,k} 2\delta(\epsilon_{nk} - \epsilon_{\text{F}})(e_\alpha \frac{\partial \epsilon_{nk}}{\partial k})(e_\beta \frac{\partial \epsilon_{nk}}{\partial k}) \qquad (3)$$

where Γ is the electron inverse life-time. Within the independent particle picture, electron lifetime is infinite and Γ is zero. However, in a real metal, material electron scatterings from electron–electron, electron–phonon and electron-defect interactions may result in a finite Γ which is also frequency dependent [28, 29]. The determination of Γ is beyond the capability of the DFT-RPA calculation and thus we only calculated the intraband Drude plasma frequency of the films.

In equations (1) and (3) the normalization volume used by the VASP package is the supercell volume (V_{sc}), which depends on the vacuum length we choose. However, for the dielectric functions ε_2 presented in this work, we first multiplied $\varepsilon_2(\text{VASP})$ directly from VASP calculations by V_{sc} and then divided by the nominal film volume ($V_{\text{fl}} = N_{\text{fl}} \times V_{1\text{ML}}$), where N_{fl} is the film thickness in units of monolayer and $V_{1\text{ML}}$ is the volume of one Al atomic layer in the corresponding bulk. That is, $\varepsilon_2 = \varepsilon_2(\text{VASP}) \times V_{\text{sc}}/(N_{\text{fl}} \times V_{1\text{ML}})$. Because $V_{1\text{ML}}$ is constant, ε_2 is equivalently normalized as per atomic layer, which does not bring in arbitrariness even though the film volume is not as strictly well defined as bulk. The interband transitions and intraband damping induced optical absorption energy loss per unit volume is proportional to the imaginary part of the dielectric function [30].

3. Results and discussion

Bulk Al has a high intraband Drude plasma frequency of about 12.4 eV and its dielectric properties as a function of incident photon energy were studied in previous papers [31]. The most striking feature from the imaginary part of the dielectric function is that it has two interband absorption peaks around 0.5 eV and 1.5 eV due to the transitions between parallel bands with energy difference of 0.5 eV and 1.5 eV, respectively. In Al(1 1 1), the interlayer distance and the half electron Fermi wavelength have a simple ratio of about 4:3, suggests a strong QSE [32], similar to the case of Pb(1 1 1) thin film with a ratio close to 3:2 [2]. We expect quantum manifestations in the plasma frequency and interband transitions will appear in Al(1 1 1) ultrathin films. To illustrate the possible QSE, we first calculated surface energy and surface stress as a function of film thickness, as shown in figure 1. Clearly, surface energy in figure 1(*a*) displays an oscillation with a 3 ML periodicity
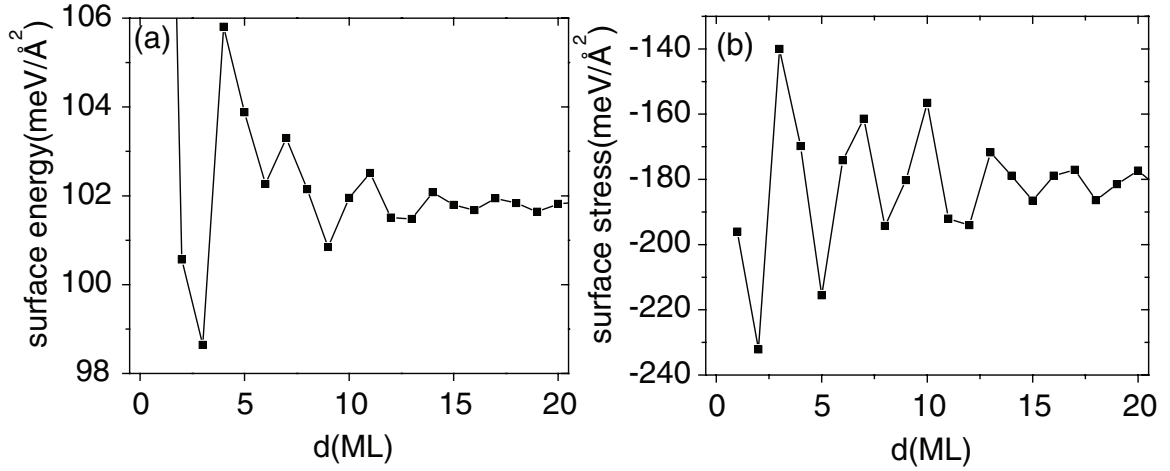
Figure 1. (*a*) Surface energy of free-standing Al(1 1 1) film as a function of thickness in units of monolayer; (*b*) the corresponding surface stress.
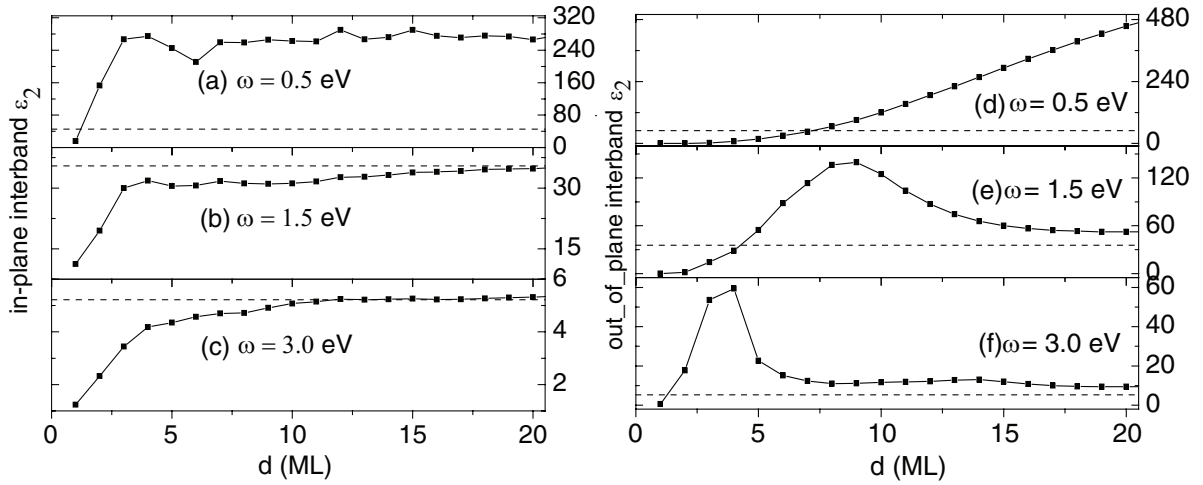
Figure 2. The imaginary part of interband in-plane dielectric function at three different energies: (*a*) $\omega = 0.5$ eV; (*b*) $\omega = 1.5$ eV; (*c*) $\omega = 3.0$ eV. The imaginary part of interband out-of-plane dielectric function at three different energies: (*d*) $\omega = 0.5$ eV; (*e*) $\omega = 1.5$ eV; (*f*) $\omega = 3.0$ eV. The dashed lines indicate the corresponding bulk values.

superimposed on a 10 ML beating pattern, especially for the first 20 MLs, in good agreement with previous result [33]. The 3 ML periodicity corresponds to the film thickness at which the electron forms a standing-wave, and the 10 ML beating pattern arises from the imperfect matching between interlayer distance and half Fermi wavelength. Surface stress displays also a QSE-induced oscillation [5], as showed in figure 1(*b*).

Next, we show the imaginary part of the in-plane and out-of-plane interband dielectric functions ε_2 as a function of film thickness for three different energies ($\omega = 0.5$ eV, 1.5 eV and 3.0 eV) in figures 2(*a*)–(*f*), respectively. The dashed line in each plot represents the corresponding bulk value. For both the in-plane and out-of-plane caseswith $\omega = 0.5$ eV at large thickness, ε_2 is much larger than the bulk value. However, for $\omega = 1.5$ eV and $\omega = 3.0$ eV, the value at large thickness is very close to the bulk value. The difference of ε_2 between the bulk and the film is due to the extra interband transitions in the film between the surface modified bulk states and between bulk states and surface states [34, 35], which are absent in the bulk.

From equation (1), it is seen that the interband ε_2 is inversely proportional to ω^2, thus the extra interband transitions give rise to larger values at the low energies and smaller values at higher energy (this trend will be more clear from the dielectric function plot in figure 3 below).

Quantum confinement is stronger at small thickness than at larger thickness, so that the energy spacing at small thickness is larger than at larger thickness. Specifically, for small thickness, the energy spacing between the initial and final states in optical transitions does not match the photon energy ω (0.5 eV, 1.5 eV and 3.0 eV) at most k-points. Consequently, the joint density of states $\delta(\epsilon_{mk} - \epsilon_{nk} - \omega)$ is very small, which gives rise to a very small ε_2 at the thicknesses less than 5 ML. As the film thickness increases, quantum confinement becomes weaker and more transitions with an energy spacing of ω become available, leading to an overall increase of the in-plane interband ε_2. Because the wavefunction is strongly modulated by quantum confinement in the direction perpendicular to the surface, the out-of-plane interband ε_2 is expected to be affected by electron transition strength $|P_{z;m,n,k}|^2$ in addition to the joint density
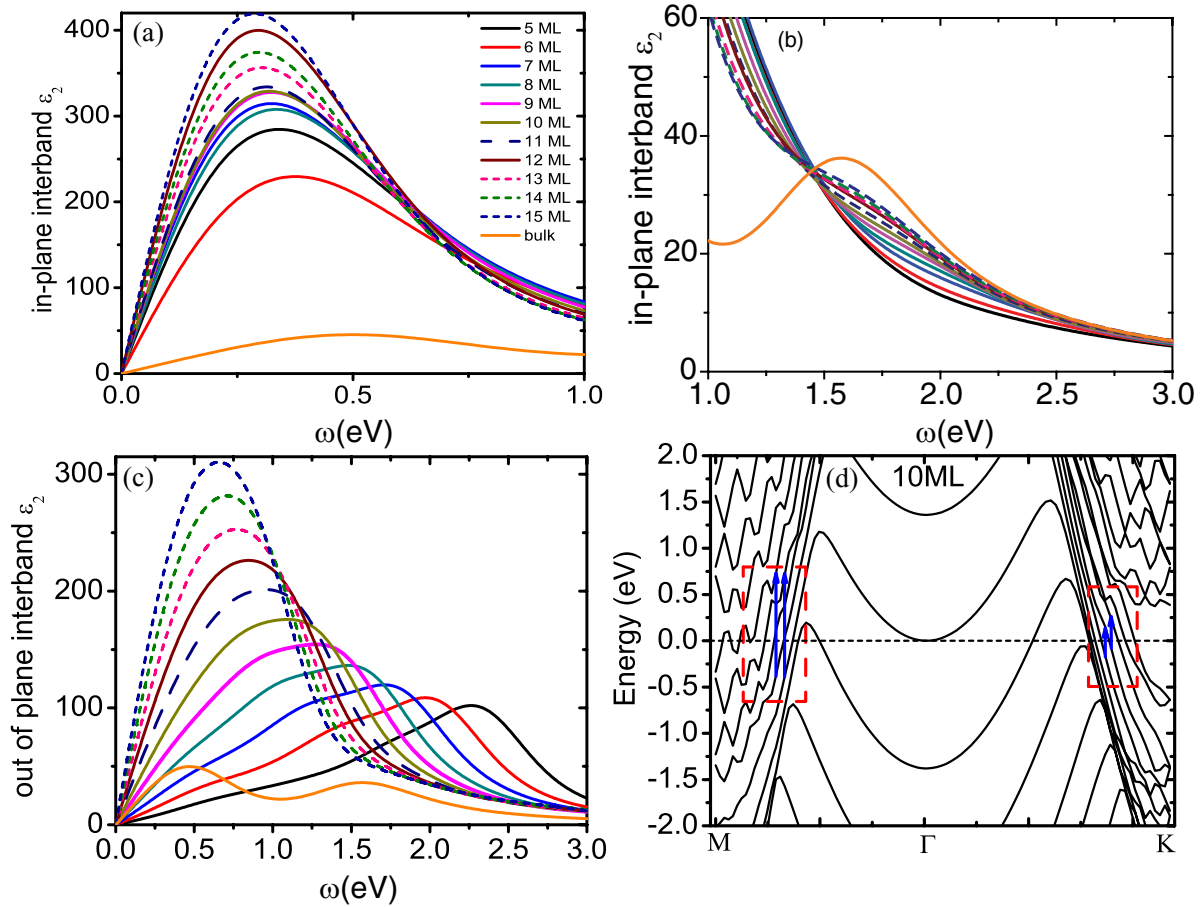
Figure 3. Imaginary part of the interband in-plane dielectric function of Al(1 1 1) films with thicknesses from 5 ML to 15 ML (*a*) at low energy range and (*b*) relatively high energy range. (*c*) The imaginary part of the interband out-of-plane dielectric function. For comparison, the bulk curve of the dielectric function is also plotted in (*a*)–(*c*). (*d*) Band structure of the 10 ML AL(1 1 1) film is shown in order to track the optical transitions responsible for the peaks in its dielectric functions. The short arrows indicate the possible transitions between two parallel bands of ~0.3 eV energy difference and the long arrows indicate the possible transitions between two parallel bands of ~1.0 eV energy difference.

of states $\delta(\epsilon_{mk} - \epsilon_{nk} - \omega)$. The thickness modulation of both $|P_{z;m,n,k}|^2$ and $\delta(\epsilon_{mk} - \epsilon_{nk} - \omega)$ may give rise to the different thickness dependence of the out-of-plane interband ε_2 in comparison with the in-plane interband ε_2. Also, because optical absorption loss is proportional to ε_2, the lower in-plane ε_2 indicates lower absorption loss. It suggests that the ultrathin film configuration can potentially be used to achieve lower loss plasmonic devices in visible and UV frequency with in-plane electric poloarization.

In figure 3 we plot ε_2 for film thickness from 5 MLs to 15 MLs together with the bulk interband ε_2 for comparison. Figures 3(*a*) and (*b*) show the low energy part ($\leqslant 1.0$ eV) and high energy part ($\geqslant 1.0$ eV) of the in-plane interband ε_2, respectively. In the low-energy range it is up to 10 times larger than the bulk value. Also, it has a red-shifted peak position from the 0.5 eV peak of bulk Al. For example, the peak moves to ~0.28 eV for the thickness of 15 MLs. Similarly in figure 3(*c*) the out-of-plane ε_2 exhibits a redshifted peak with enhanced magnitude compared to the peak of the bulk at 1.5 eV. The red-shifted and enhanced peak is related to the film band structure. We have plotted the band structure of the 10 ML film as a representative thickness in figure 3(*d*). Around the Fermi energy, parallel bands with energy differences of

0.3 eV and 1.0 eV are found, which are indicated by short and long arrows, respectively. The peak around 0.3 eV in the in-plane dielectric function plot for the 10 ML film in figure 3(*a*) is due to transitions in the parallel bands with energy difference of 0.3 eV. The peak around 1.0 eV in the out-of-plane dielectric function plot for the 10 ML film in figure 3(*c*) is due to transitions in the parallel bands with an energy difference of 1.0 eV. Consistent with figures 2(*a*)–(*c*), overall the in-plane ε_2 increases with film thickness to the final converged value. On the other hand, the out-of-plane ε_2, as shown in figure 3(*c*), also increases with film thickness for frequencies less than ~0.75 eV. Thus, we expect that ultrathin films could be utilized for low-loss plasmonic devices with an in-plane and/or out-of-plane electric polarization.

Next, we calculated the in-plane intraband Drude plasma frequency ω_{pl} as a function of film thickness, as shown in figure 4(*a*), which shows the film thickness dependence of intraband contribution to the dielectric function as defined in equation (2). First, there is a very fast decay of ω_{pl} from 14.3 eV to 10.5 eV going from 1 ML to 3 ML film. Second, there also appears a 3 ML oscillation pattern with quickly decaying amplitude in ω_{pl}. To understand these observations, we noticed
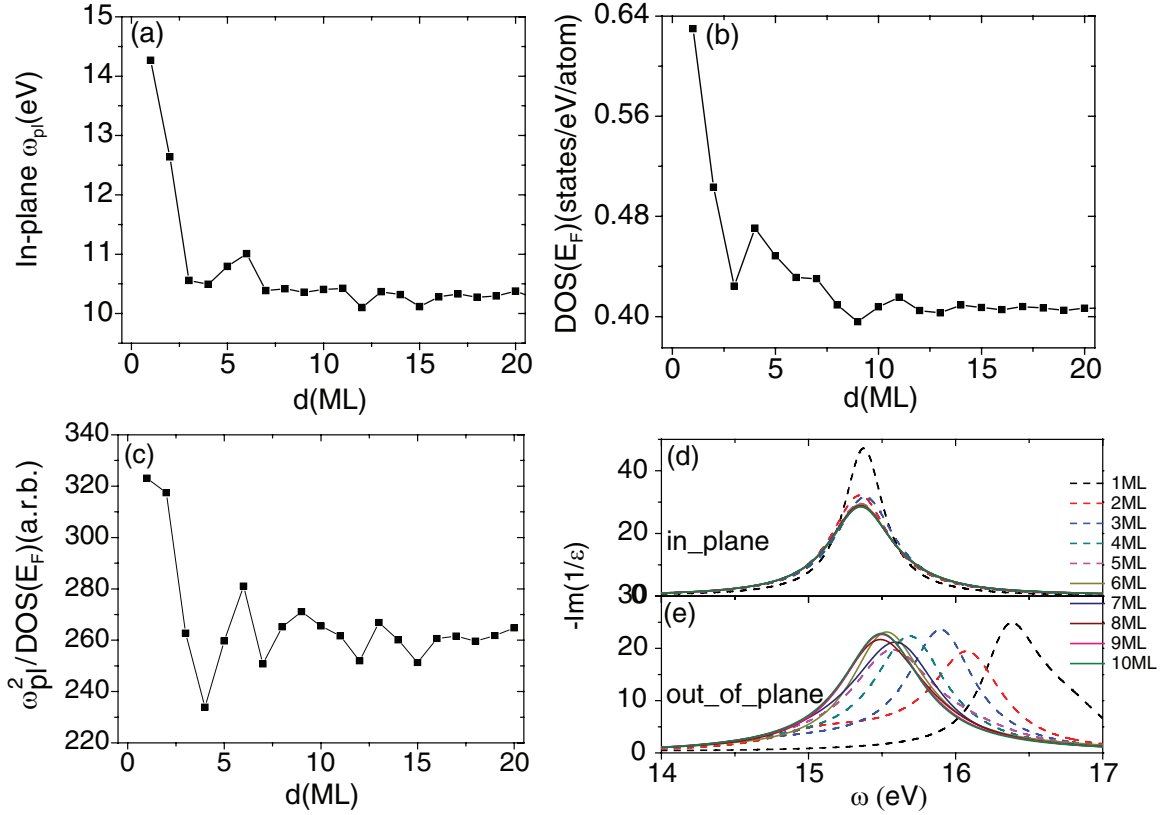
Figure 4. (*a*) The slab plasma frequency (in eV) as a function of Al(1 1 1) film thickness. The dashed line indicates the bulk plasma frequency. (*b*) Electron density of states (DOS) at the Fermi energy as a function of film thickness. (*c*) $\omega_{pl}^2/\mathrm{DOS}(E_F)$, showing the dependence of average $\frac{\partial \epsilon_{nk}}{\partial k}$ on film thickness. (*d*) In-plane energy loss function and (*e*) out-of-plane energy loss function for thicknesses from 1 ML to 10 ML.

from equation (3) that the squared ω_{pl} is proportional to the electron density of states (DOS) at the Fermi energy if $e_\alpha \frac{\partial \epsilon_{nk}}{\partial k}$ varies slowly with k or remains constant. Therefore, we calculated the DOS at the Fermi energy at different film thickness in figure 4(*b*). It shows a similar oscillation pattern as the Drude plasma frequency in figure 4(*a*). In particular, the DOS drops significantly from the 1 ML, 2 ML to 3 ML film and then converges quickly with further increasing film thickness. We thus attributed the large plasma frequency of the ultrathin 1 ML, 2 ML and 3 ML films to their large DOS at the Fermi energy. However, the oscillation pattern of plasma frequency does not match exactly in a one-to-one fashion to that of DOS at the Fermi energy. This may be related to the modulation of $\frac{\partial \epsilon_{nk}}{\partial k}$ term in equation (3) by QSE, which is also thickness dependent. In order to see the effect of $\frac{\partial \epsilon_{nk}}{\partial k}$ on ω_{pl}, we have plotted $\omega_{pl}^2/\mathrm{DOS}(E_F)$, which is proportional to $\frac{\partial \epsilon_{nk}}{\partial k}$, as a function of film thickness in figure 4(*c*). It shows strong oscillation with film thickness. We may attribute the different oscillation patterns in figure 4(*a*) versus in figure 4(*b*) to the effect of $\frac{\partial \epsilon_{nk}}{\partial k}$.

We realized that the plasma frequency defined in equation (3) is the same as the Drude plasma frequency. However, only in a free electron gas are there intraband transistions without interband transitions. In real materials, there are also interband transitions, so the plasma frequency is determined by both intraband and interband dielectric functions. Therefore, the Drude plasma frequency as

calculated here, which includes only intraband transitions, does not represent the physical collective excitation energy [29]. Instead, the collective excitation plasma frequency can be determined by the peak positions in the energy loss function (ELF) spectrum, defined as [36]: ELF = $\mathrm{Im}(-1/\varepsilon) = \varepsilon_2/(\varepsilon_1^2 + \varepsilon_1^2)$. We thus plotted the ELF for thicknesseses of Al(1 1 1) film from 1 ML to 10 ML in figures 4(*c*)–(*d*). Figure 4(*c*) is the in-plane ELF and (*d*) is the out-of-plane ELF. The peak positions converge quickly to 15.3 eV, in good agreement with the bulk Al plasma frequency calculated previously [31], as well as with our calculated bulk value.

We note that our calculated Drude plasma frequency of bulk Al is 12.4 eV, in good agreement with previous studies [31]. However, the in-plane Drude plasma frequency of Al(1 1 1) film in figure 4(*a*), which is well converged at film thickness greater than 10 ML, is ~2 eV, noticeably smaller than the bulk value. Similar discrepancy has been previously reported for Cu(1 1 0) [21], Au(1 1 1) [17] and Ag(1 1 0) [37]. This might be partly due to the surface termination, which perturbs the bulk wave-functions to give rise to repeating bands crossing the Fermi energy, and nonzero interband transition strength from bands below the Fermi energy to those bands crossing the Fermi energy. Consequently, a reduction of intraband Drude plasma frequency results in the thin film. From [38], the mathematical proof that the film intraband Drude plasma frequency is smaller than the bulk intraband

Drude plasma frequency shows that:

$$\omega_{\alpha\alpha}^2 = \frac{8\pi e^2 \hbar^2}{V m^2} \sum_{n-pf} \sum_{m \neq n} 2 f_{nk} \frac{|\langle u_{mk} | (k_a - i\nabla_a) | u_{nk}\rangle|^2}{\varepsilon_{nk} - \varepsilon_{mk}}$$
$$+ \frac{4\pi e^2 n \hbar^2}{m} \tag{4}$$

where 'n-pf' indicates that band *n* is partially occupied and *m* is un-occupied. So $\varepsilon_{nk} - \varepsilon_{nk} < 0$ and the first term on the right hand side of the above equation is always negative. The increased interband transitions from bands below Fermi the energy to the bands crossing the Fermi energy will decrease the first term, so that the resulting thin film value is smaller than the bulk value.

Experimentally Si(1 1 1) [32] and GaAs(1 0 0) [39] substrates were used to epitaxially grow ultrathin Al film. In general, a substrate may exert both strain and charge transfer effects on the overlayer thin film, e.g. causing a phase shift in the quantum-size-effect induced oscillation pattern [5]. In addition, one may speculate that surface roughness may also affect the electronic properties of the overlayer film, changing plasma frequencies and optical inter-band transitions. These are interesting subjects of future studies.

4. Conclusion

We performed DFT calculations of the dielectric function of free-standing Al(1 1 1) ultrathin films of thickness from 1 to 20 MLs with RPA. Both the intraband and interband contributions to the total dielectric function were shown to be modulated by QSE through the calculation of the imaginary part of the interband dielectric function and slab intraband Drude plasma frequency. Overall, the in-plane components (interband transition) of ε_2 increase with film thickness at all frequencies, and convergetowards a constant value. The out-of-plane components of ε_2 show complex behavior, and only at frequencies less than 0.75 eV does ε_2 increase with film thickness, but without convergence. This finding suggests that ultrathin films can potentially be used for low-loss plasmonics devices in the visible and UV range. Our results may shed light on the search for low absorption-loss plasmonic materials through electronically tuning the band structure of metallic films by using different thicknesses.

Acknowledgments

References

[1] Liu F, Khanna S N and Jena P 1990 *Phys. Rev.* B **42** 976
[2] Luh D-A, Miller T, Paggel J J, Chou M Y and Chiang T-C 2001 *Science* **292** 1131
[3] Hong H, Wei C-M, Chou M Y, Wu Z, Basile L, Chen H, Holt M and Chiang T-C 2003 *Phys. Rev. Lett.* **90** 076104
[4] Hu H, Gao H and Liu F 2012 *Phys. Rev. Lett.* **109** 106103
[5] Liu M, Han Y, Tang L, Jia J-F, Xue Q-K and Liu F 2012 *Phys. Rev.* B **86** 125427
[6] Wang L L, Ma X C, Jiang P, Fu Y S, Ji S H, Jia J F and Xue Q K 2007 *J. Phys.: Condens. Matter* **19** 306002
[7] Ma L-Y *et al* 2006 *Phys. Rev. Lett.* **97** 266102
[8] Ma X, Jiang P, Qi Y, Jia J, Yang Y, Duan W, Li W-X, Bao X, Zhang S B and Xue Q-K 2007 *Proc. Natl Am. Sci.* **104** 9204
[9] Kim J, Qin S, Yao W, Niu Q, Chou M Y and Shih C-K 2010 *Proc. Natl Am. Sci.* **107** 12761
[10] Liu M and Liu F 2014 *Nanotechnology* **25** 135706
[11] West P, Ishii S, Naik G, Emani N, Shalaev V and Boltasseva A 2010 *Laser Photon. Rev.* **4** 795
[12] Politano A, Formoso V and Chiarello G 2013 *J. Phys.: Condens. Matter* **25** 305001
[13] Novotny L and van Hulst N 2011 *Nat. Photon.* **5** 83
[14] Dryzek J and Czapla A 1987 *Phys. Rev. Lett.* **58** 721
[15] Apell P and Ahlqvist P 1981 *Phys. Scr.* **22** 659
[16] Xiao M, Villagomez R and Alvarez L 2000 *J. Phys.: Condens. Matter* **12** 2925
[17] Laref S, Cao J, Asaduzzaman A, Runge K, Deymier P, Ziolkowski R W, Miyawaki M and Muralidharan K 2013 *Opt. Express* **21** 11827
[18] Kuzik L A, Yakovlev V A, Pudonin F A and Mattei G 1996 *Surf. Sci.* **361** 882
[19] Kuzik L A, Yakovlev V A, Pudonin F A and Yakovlev V A 1994 *JETP* **78** 114
[20] Bobb D A *et al* 2009 *Appl. Phys. Lett.* **95** 151102
[21] Harl J, Kresse G, Sun L D, Hohage M and Zeppenfeld P 2007 *Phys. Rev.* B **76** 035436
[22] Park C-H, Spataru C D and Louie S G 2006 *Phys. Rev. Lett.* **96** 126105
[23] Yang L 2011 *Nano Lett.* **11** 3844
[24] Bruno M, Palummo M, Marini A, Del Sole R, Olevano V, Kholod A N and Ossicini S 2005 *Phys. Rev.* B **72** 153310
[25] Kresse G and Joubert D 1999 *Phys. Rev.* B **59** 1758
[26] Perdew J P, Chevary J A, Vosko S H, Jackson K A, Pederson M R, Singh D J and Fiolhais C 1992 *Phys. Rev.* B **46** 6671
[27] Kresse G and Furthmuller J 1996 *Phys. Rev.* B **54** 11169
[28] Cazzaniga M, Caramella L, Manini N and Onida G 2010 *Phys. Rev.* B **82** 035104
[29] Kaltenborn S and Schneider H C 2013 *Phys. Rev.* B **88** 045124
[30] Yang L, Deslippe J, Park C-H, Cohen M L and Louie S G 2009 *Phys. Rev. Lett.* **103** 186802
[31] Lee K-H and Chang K J 1994 *Phys. Rev.* B **49** 2362
[32] Flötotto D, Wang Z, Jeurgens L P H and Mittemeijer E J 2012 *Phys. Rev. Lett.* **109** 045501
[33] Han Y and Liu D-J 2009 *Phys. Rev.* B **80** 155404
[34] Manghi F, Del Sole R, Selloni A and Molinari E 1990 *Phys. Rev.* B **41** 9935
[35] Manghi F, Molinari E, Del Sole R and Selloni A 1989 *Phys. Rev.* B **39** 13005
[36] Yan J, Mortensen J J, Jacobsen K W and Thygesen K S 2011 *Phys. Rev.* B **83** 245122
[37] Monachesi P, Palummo M, Del Sole R, Ahuja R and Eriksson O 2001 *Phys. Rev.* B **64** 115421
[38] Harl J 2008 The linear response function in density functinal theory: optical spectra and improved description of the electron correlation *PhD Dissertation* Universitat Wien, chapter 2
[39] Lin S-W, Wu J-Y, Lin S-D, Lo M-C, Lin M-H and Liang C-T 2013 *Japan J. Appl. Phys.* **52** 045801